Airfoil Design Method Using the Navier-Stokes Equations

J. B. Malone*
NASA Langley Research Center, Hampton, Virginia 23665
J. C. Narramore†
Bell Helicopter Textron, Inc., Ft. Worth, Texas 76101
and
L. N. Sankar‡
Georgia Institute of Technology, Atlanta, Georgia 30332

An airfoil design procedure is described that has been incorporated into an existing two-dimensional Navier-Stokes airfoil analysis method. The resulting design method, an iterative procedure based on a residual-correction algorithm, permits the automated design of airfoil sections with prescribed surface pressure distributions. This paper describes the inverse design method and the technique used to specify target pressure distributions. It presents several example problems to demonstrate application of the design procedure. These examples illustrate that the inverse design method can be used to develop useful airfoil configurations with a reasonable expenditure of computer resources.

Introduction

THE aerodynamic design of aircraft components is often carried out by means of one of the following four approaches: 1) "cut-and-try" analysis, 2) indirect methods, 3) optimization techniques, and 4) inverse design techniques. The cut-and-try approach consists of multiple applications of direct aerodynamic analysis methods. The design engineer specifies a geometry and then uses the computed flowfield to guide further changes to the geometry definition. This approach to aerodynamic design is time consuming and usually requires considerable expertise to produce optimum configurations. Unlike the cut-and-try method, the latter three design techniques are far more automated, requiring fewer "engineer-in-the-loop" interactions to achieve specific design goals. These automated design methods can reduce the overall engineering effort and calendar time for developing aircraft components and configurations that have favorable aerodynamic performance or aerodynamic interference characteristics. A variety of different analytical and numerical design algorithms has been developed, and Sloof has summarized a number of the most successful methods in Ref. 1.

Automated design methods of the "design-to-pressure" type are normally used to generate aerodynamic geometries that have favorable surface pressure distributions at given freestream conditions. For example, high-speed aircraft lifting-surface geometries that generate "shock-free" or "weak-shock" flowfields are usually sought to minimize wave drag performance penalties. Obviously, the use of these automated design methods requires that the aerodynamicist can specify, a priori, the desired pressure distribution for a particular application.

By far the most widely used aerodynamic design procedures are based upon potential-flow computational fluid dynamic (CFD) methods.[1,2-5] Although it is likely that potential-flow design procedures will continue to be used as the "workhorses" in industry due to their relatively low cost in terms of computer-resource requirements, there is now an increasing interest in developing similar design procedures that use higher order CFD methods such as the Euler equations[6-8] and the Reynold-averaged Navier-Stokes equations.[9] If used during the design process, these higher order CFD methods help the aerodynamicist to account for the occurrence of fluid dynamic effects or phenomena that are not routinely predictable using potential-flow methods

In Ref. 10, Garabedian and McFadden described an inverse aerodynamic design procedure that they demonstrated using an existing full-potential equation (FPE) aerodynamics code. Their design method is based on a residual-correction algorithm, which we will refer to here as the GM method, and can be used to generate aerodynamic surfaces with prescribed surface pressure distributions. In Ref. 11, Malone et al. presented a Modified Garabedian-McFadden (MGM) design algorithm that removed some limitations of the original GM technique. These authors applied the new MGM design method, also using FPE aerodynamic analysis codes as a basis, to airfoil, axisymmetric nacelle inlet, and three-dimensional nacelle inlet design problems. Later, Hazarika[12] and Sankar used an FPE CFD method to apply the MGM procedure to the design of blended wing-body configurations. In a recent effort, Malone et al.[13] described the first use of the MGM residual-correction design algorithm coupled with a two-dimensional Navier-Stokes solution procedure. Subsequently, a similar viscous-flow design procedure was presented by Birckelbaw.[14]

The objective of the present research was to develop a design method for viscous, attached-flow design problems that might be beyond the capability of potential-flow or Euler methods, even those using interactive boundary-layer theories. Because the aerodynamic designer normally seeks attached-flow conditions, the method described in Ref. 13 was not expected to handle separated-flow design problems. However, by virtue of the fact that a Navier-Stokes method forms the basis of the present procedure, the possible occurrence and extent of separated-flow regions can be directly computed during the design process.

Received July 29, 1989; revision received March 22, 1990.

*Head, Unsteady Aerodynamics Branch. Associate Fellow AIAA.
†Principal Engineer, Aerodynamic Technology. Member AIAA.
‡Associate Professor, School of Aerospace Engineering. Member AIAA.

The present paper summarizes the Navier-Stokes inverse design method originally presented in Ref. 13. The paper describes the two-dimensional Navier-Stokes computational procedure, the MGM design algorithm, implementation of the design procedure and the technique used to define target pressure distributions, and also presents the results of several sample airfoil design problems

Navier-Stokes Solution Procedure

The two-dimensional Navier-Stokes procedure used in the present work was originally developed by Sankar and Tang[15] and later extended by Huff and Sankar.[16] Their method solves the Reynold-averaged form of the full Navier-Stokes equations using a generalized coordinate transformation and a body-fitted computational grid. The mathematical formulation in generalized coordinates consists of a nondimensionalized set of equations cast in a strong conservative form:

$$Q_t + D_\xi + E\eta = M_\infty R_e^{-1} (G_\xi + H\eta) \qquad (1)$$

In Eq. (1), Q is the vector of conserved flow variables, which are themselves combinations of the usual primative variables, density ρ, the components of fluid velocity u, v, and the fluid total energy e. The quanity M_∞ is the freestream Mach number, and R_e is the Reynolds number. The vectors D and E are the inviscid flux vectors in the ξ and η coordinate directions, respectively. Also, the vectors G and H are the viscous flux terms in the corresponding coordinate directions. The techniques used to solve Eq. (1) are given in Refs. 15 and 16. Here we present only a brief description of the Navier-Stokes solution procedure.

The Navier-Stokes system of equations given by Eq. (1) is solved on a structured mesh by means of a finite-difference technique. The system of equations is integrated in time with the implicit Beam-Warming algorithm.[17] Second-order finite-difference expressions are used for spatial derivatives, whereas first-order differences are used for temporal terms. Also, a combination of second- and fourth-order artifical dissipation is added for numerical stability. The procedure models the viscous stress terms in an explicit manner by keeping these terms on the right side of the equation. For the present work, the Baldwin-Lomax[18] algebraic eddy viscosity model was used to simulate turbulent flowfield effects. Finally, the computational grid used in the present application is a C-grid topology, with the ξ coordinate in the wraparound direction and the η coordinate in surface normal direction. The C-grid is generated algebraically with the sheared-parabolic technique. For the present design applications, this type of algebraic grid generation procedure is desirable because it is extremely fast and computationally efficient.

MGM Design Procedure

The MGM design method can be classified as a residual-correction technique in which the residuals are the difference between the desired speed distribution and the computed distribution. Over the past decade a number of residual-correction methods have been developed, such as the "wavy-wall" approach of Davis.[19] The methods differ primarily in the manner in which changes in residual are related to changes in surface shape. The MGM algorithm itself consists of an auxiliary partial differential equation (PDE) that is solved for incremental changes in surface coordinates during each design cycle. The final aerodynamic shape is approached in a stepwise fashion through a cyclical iteration between the flow solver and the MGM algorithm.

Mathematical Formulation

For two-dimensional flow about an airfoil configuration, the MGM auxiliary equation is given by

$$F_0 S_t + F_1 S_{xt} + F_2 S_{xxt} = R \qquad (2)$$

where R is the residual, defined as $R = q_c^2 - q_t^2$, the quantities q_c and q_t are the computed and target speed distributions, the coordinate x is the usual Cartesian coordinate taken here to lie along the airfoil chordline, and the coefficients F_0, F_1, and F_2 are constants chosen to provide a stable iterative process. Figure 1 shows how this auxiliary equation is typically incorporated into existing flow solution procedures. The computed surface velocities are normally obtained from partially converged numerical solutions to the flow equations under consideration at a given value of time t. For the purpose of obtaining computed values, these flow equations may be solved in either a time-accurate or variable time-stepping manner. During the design process, as q_c approaches q_t, the right side of Eq. (2) vanishes, and subsequent solutions of this auxiliary equation yield minimal changes in the airfoil surface coordinates.

Next, Eq. (2) is written in terms of a correction to the airfoil coordinates ΔS by using the temporal derivatives and choosing $\Delta t = 1$, so that Eq. (2) can then be written as

$$F_0 \Delta S + F_1 (\Delta S)_x + F_2 (\Delta S)_{xx} = R \qquad (3)$$

The present inverse design procedure is formulated in a manner similar to that of the original GM scheme but with

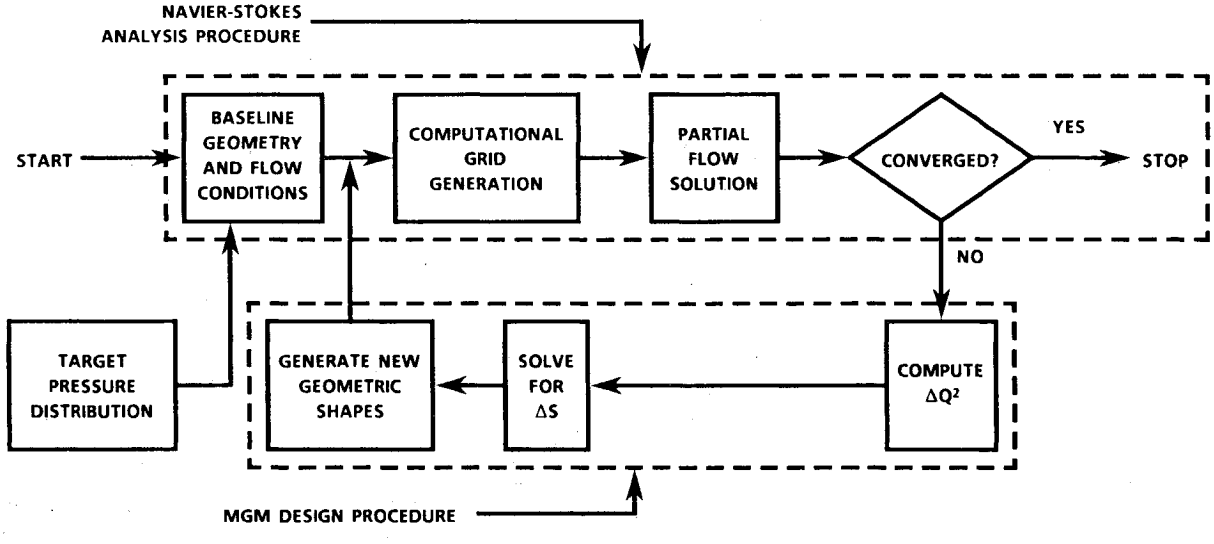

Fig. 1 Implementation of the MGM inverse design algorithm.

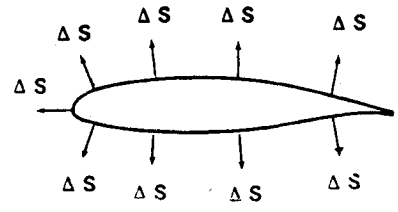

a) Original Garabedian-McFadden method

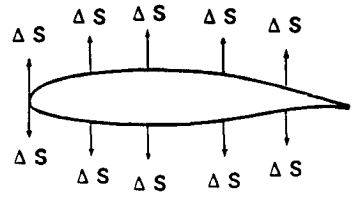

b) Modified Garabedian-McFadden method

Fig. 2 Schematic of geometry perturbations for original (GM) and modified (MGM) inverse design algorithms.

several important differences. In the MGM method, the auxiliary equation is solved directly in the physical domain rather than in the computational domain, as was done in Ref. 10. Additionally, whereas the GM method was recommended for use only on a portion of the airfoil surface, excluding the leading and trailing edges,[10] and then only with an increase in the airfoil thickness away from some thinner starting configuration,[1] the MGM design algorithm was developed as an airfoil design method through which arbitrary changes to the complete airfoil geometry could be generated, including situations where modifications to the leading-edge shape are required. This capability helps to eliminate the need for a starting configuration that is close in shape to the final designed airfoil shape.

A further difference is shown in Fig. 2, where the surface perturbations generated with the MGM procedure are interpreted as changes in the coordinate direction perpendicular (y direction) to the longitudinal axis of the geometry (x direction). This choice for the movement of the surface coordinates (which differs from the original GM method) has been demonstrated to generate a smoother leading-edge geometry and eliminates chordwise stretching of the airfoil.[11]

Numerical Solution Procedure

We solve the auxiliary PDE by writing finite-difference expressions for each term of Eq. (3). The computational grid used to solve this equation is the same grid used for the fluid-dynamic equations, which, for the present Navier-Stokes solver, is an algebraically generated C-grid topology. Of course, Eq. (3) is solved only along the airfoil surface, so that only the grid-line clustering in the x or streamwise direction is of importance.

Then, assuming that there are a total of N computational points on the airfoil surface, Eq. (3) is written for each of these points where $1<i<N$. A typical equation evaluated at the ith point on the surface is

$$A_i\Delta Y_{i+1} + B_i\Delta Y_i + C_i\Delta Y_{i-1} = R_i \tag{4}$$

Here the coefficients A_i, B_i, and C_i are evaluated by means of standard finite-difference expressions, and ΔY_i is the incremental change in surface coordinate ΔS at the ith computational point. The use of the Y coordinate here results from the direction chosen for incrementing the airfoil surface. First-order-accurate, spatially upwinded derivatives are used to discretize the $(\Delta Y)_x$ terms, whereas second-order-accurate expressions are used to model the $(\Delta Y)_{xx}$ terms. Also, since Eq. (4) is solved in the physical domain, the finite-difference expressions are normally derived for nonuniform grid-point distributions in the x, or streamwise, direction.

For points on the airfoil upper surface, the following expressions are obtained:

$$A_i = -2F_2/[(x_{i+1} - x_i)(x_{i+1} - x_{i-1})] \tag{5a}$$

$$B_i = F_0 + F_1/(x_i - x_{i-1}) + 2F_2/[(x_{i+1} - x_i)(x_i - x_{i-1})] \tag{5b}$$

$$C_i = -F_1/(x_i - x_{i-1}) - 2F_2/[(x_i - x_{i-1})(x_{i+1} - x_{i-1})] \tag{5c}$$

$$R_i = R_i \tag{5d}$$

For points on the airfoil lower surface, similar expressions are derived:

$$A_i = -F_1/(x_i - x_{i+1}) - 2F_2/[(x_{i+1} - x_i) \times (x_{i+1} - x_{i-1})] \tag{6a}$$

$$B_i = F_0 + F_1/(x_i - x_{i+1}) + 2F_2/[(x_{i+1} - x_i)(x_{i+1} - x_{i-1})] \tag{6b}$$

$$C_i = -2F_2/[(x_i - x_{i-1})(x_{i+1} - x_{i-1})] \tag{6c}$$

$$R_i = -R_i \tag{6d}$$

During the derivation of Eqs. (5-6), the change in sign between slope and curvature is accounted for so that the coefficients F_0, F_1, and F_2 are assumed to be positive constants. For example, on the airfoil upper surface the appropriate proportionality to take between the slope and the residual term, F_1 $(\Delta S)_x \simeq R$, is that F_1 should be positive (locally) if $(\Delta S)_x$ and R are positive. However, for the curvature term $(\Delta S)_{xx}$, when the airfoil upper surface has a positive value of R, the airfoil should be thickened locally. This leads to a negative curvature (increase in thickness on the upper surface) and a negative F_2 term, so that the product $F_2(\Delta S)_{xx}$ will have the same sign as R. The opposite observation is true for the airfoil lower surface. This change in sign for the curvature term is accounted for in Eqs. (5) and (6) so that the factor F_2 is also considered a positive number.

Special treatment is used in the evaluation of Eq. (3) at the leading edge, where an ambiguity arises as to the direction in which to apply the upwind derivatives, especially for nonzero angle-of-attack conditions. To eliminate this problem, the leading-edge point is constrained to move as the average of both the upper and lower surface points located just downstream of the leading-edge point. This constraint is treated implicitly by the replacement of the coefficients in Eq. (4) with the following expressions:

$$A_i = -0.5 \tag{7a}$$

$$B_i = +1.0 \tag{7b}$$

$$C_i = -0.5 \tag{7c}$$

$$R_i = 0.0 \tag{7d}$$

Thus, the leading edge is free to translate vertically, allowing for relative angle-of-attack adjustments to occur naturally.

Equation (4) is evaluated at each point i around the airfoil surface, leading to a system of equations with N unknowns, the ΔY_i values. Note that at each point on the aerodynamic surface, ΔY_i is coupled to values at neighboring points. The resulting algebraic equations form a tridiagonal system that is solved for values of ΔY_i using the Thomas algorithm.[19]

The design cycle is completed by updating the previous surface geometry using the new value of ΔY_i as follows:

$$Y_i^{\text{new}} = Y_i^{\text{old}} + \Delta Y_i,\ i = 1, \ldots, N \tag{8}$$

Calculation of Target Velocity Distributions

Previous FPE applications of the MGM design procedure[11] used an expression for q^2 as a function of airfoil pressure coefficient C_p that is derived for isentropic flow. This expression is

$$q^2 = \left[1 - \left(\{C_p[(\gamma-1)/2]M_\infty^2 + 1\}^{(\gamma-1/\gamma)} - 1\right) \times 2M_\infty^2\right] \tag{9}$$

where γ is the ratio of specific heats.

Equation (9) is also used in the present Navier-Stokes design method to convert computed and target surface pressure coefficient distributions into equivalent velocity distributions. However, these are nonphysical velocity distributions, since the viscous flow is nonisentropic, and the numerical boundary conditions used in the flow solver are the usual "nonslip" conditions (i.e., $u = v = 0$). Nevertheless, the "psuedovelocity" function given by Eq. (9) has proven to be effective in the current applications of the MGM inverse design procedure. That is, the airfoil geometry perturbations computed during each design iteration are in the correct direction to generate either increases or decreases in local velocity as dictated by the residual term R.

Trailing-Edge Crossover

The present inverse procedure was developed to permit the design of complete airfoil surfaces, including the leading-edge and trailing-edge regions. However, a completely arbitrary choice for a target pressure distribution does not always result in a well-posed inverse design problem. For example, Volpe[4] has presented a technique to satisfy the three integral constraints relating target pressures and freestream conditions that are required to ensure a well-posed problem in compressible flow. As a possible consequence of using unconstrained target pressures, the inverse procedure may produce an airfoil geometry that exhibits trailing-edge crossover or leads to other unrealistic configurations.

Therefore an artifice is used in the present work so that the trailing-edge thickness can be controlled and so that any tendency of the airfoil to "fishtail" is identified. If the geometry is driven to a fishtail configuration (trailing-edge crossover), a linear wedge is removed from the airfoil section so that the resulting trailing-edge thickness equals a predetermined value. In applying the wedge technique, surface modifications are made equally to both the upper and lower surfaces. These modifications are linearily varying from zero at the leading edge to a maximum of one-half the desired trailing-edge thickness at the airfoil trailing edge. If no crossover occurs on the airfoil surface, but the designer wants to fix the trailing-edge thickness to some predetermined value, a wedge is either removed or added to enforce this constraint. Otherwise, the designed geometry remains as produced by the MGM algorithm without postprocessing modifications. It has been demonstrated that this wedge technique can give some measure of control over the potential manufacturability of airfoil configurations generated by automated design procedures.[21] It should be noted that if the preceding wedging technique is required continuously during the design process, the original target pressures should be examined for possible modification along the lines discussed by Volpe.[4]

Design Convergence Considerations

As in other iterative inverse design methods or design procedures based on optimization methods, formal convergence criteria are somewhat arbitrary. That is, the design engineer usually decides case by case how close the new airfoil must come to achieving the target pressure goals. Also, as mentioned, the target pressures themselves may not always produce a manufacturable airfoil geometry. For these reasons, the design engineer should be able to monitor the progress of the design method while it is generating a new airfoil shape.

The present design procedure has been structured to facilitate its use as a multistep procedure, allowing the design engineer to monitor the results of each step before proceeding with a subsequent computer submittal. Of primary concern to the engineer are data that measure the "closeness" of the current computed pressures to the targets. The following information can be used to monitor the progress of the iterative design procedure: the location and value of the maximum residual term $R_{\max}$, the computed and target C_p values corresponding to $R_{\max}$, the average R value around the airfoil surface, and the average $\Delta C_p = \text{abs}(C_{p_t} - C_{p_c})$ around the airfoil surface.

Direct control over the maximum number of iterations per program execution, the number of flow solver ADI iterations between surface geometry updates, and the maximum value of ΔY_i permitted along the airfoil are also incorporated in the present design procedure. The importance of the first item mentioned is obvious. The second feature allows the user some control over the accuracy of the computed C_p values. Each sequence of ADI iterations defines one design cycle, and the more iterations used per design cycle, the better will be the approximation of C_{p_c} for the current airfoil geometry. The latter item permits the program user to control the speed of the design process by limiting the magnitude of the airfoil surface updates. This control can also be used to limit any possible adverse effects that might arise from the inadvertent use of inappropriately low values of F_0, F_1, and F_2.

Target Pressure Selection

One approach to selecting target pressure distributions that satisfy prescribed performance objectives is described in Ref. 22. This method is incorporated into a computerized aerodynamic design and analysis system called ADAM. The ADAM

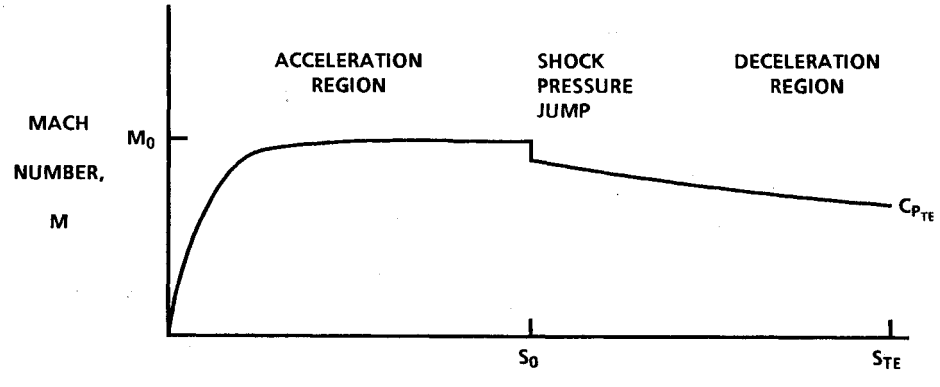

Fig. 3 Parametric equations defining the Mach number distribution along the surface of an airfoil.

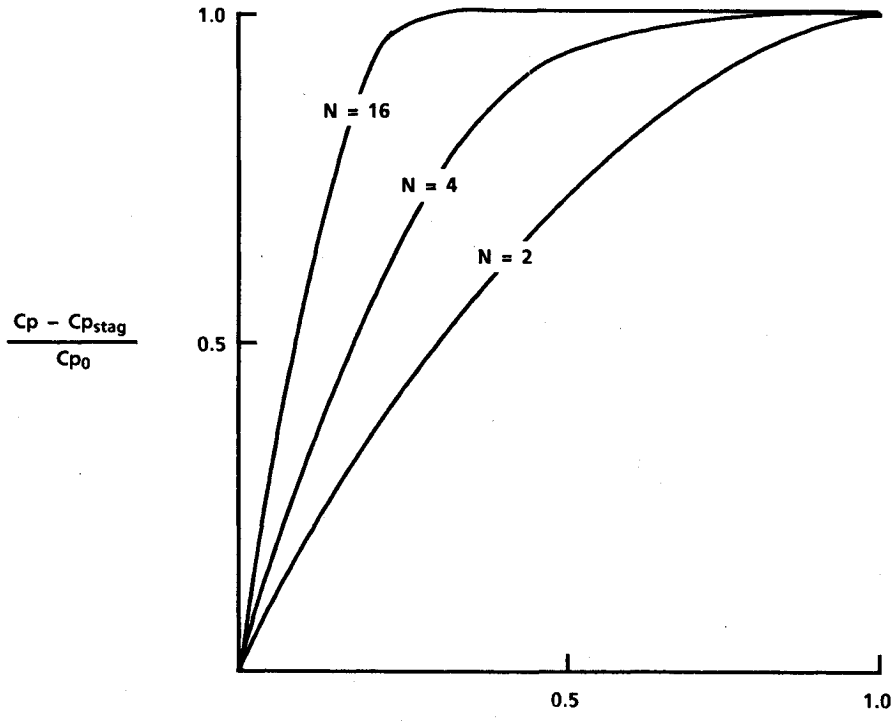

Fig. 4 Effect of the parameter n on acceleration region distribution.

system is described in the following paragraphs for the sake of completeness.

The approach taken in the ADAM transonic airfoil design methodology is to assume generalized equations for the target velocity distribution along the perimeter of the airfoil. Advantages stem from the fact that there exists a series of expressions with a small number of coefficients that may be varied to determine the velocity distribution that will best satisfy the lift, drag, and pitching moment requirements at the design point conditions. These parameters may be systematically varied to produce families of velocity distribution curves from which the best velocity distribution to satisfy the design requirements may be selected. This approach can significantly reduce the effort required to determine the target pressure distribution for input to an inverse design code.

Velocity Distribution Equations

The ADAM system evaluates families of velocity distributions to determine which distribution on the airfoil will best satisfy the performance requirements. On the upper and lower surface of the airfoil, the velocity distribution is divided into an acceleration region with one equation, a deceleration region with a second equation, and a shock pressure jump between them if the flow in the acceleration region becomes sonic. These three regions are indicated schematically in Fig. 3.

Acceleration Region

The pressure distribution in the acceleration region is of the form

$$C_p = C_{p_s} + (C_{p_0} - C_{p_s})\,[1 - (1 - S_a/S_0)^n] \qquad (10)$$

where C_{p_0} is the pressure coefficient at the location S_0 of the peak Mach number, S_a is the airfoil surface length measured from the stagnation point, and C_{p_s} is the stagnation pressure coefficient. As Fig. 4 shows, increasing the value of n in this equation drives the Mach number to a rooftop distribution and allows for airfoils with different nose radii.

Shock Pressure Rise

If the peak Mach number M_0 is greater than one, a shock will form at the start of the pressure recovery. Yoshihara[23] indicates that the pressure behind the shock on an airfoil may be estimated by a value that is halfway between the pressure associated with sonic flow behind an oblique shock and an oblique shock detachment. Then an effective wedge angle Δ can be established as

$$\Delta = [0.148(M_0^2 - 1)^{3/2} + 0.1604(M_0^2 - 1)^{3/2}]/M_0^2 \qquad (11)$$

and used to estimate the pressure rise through the shockwave:

$$P_j = 1 + \gamma M_0^2 \Delta/\beta + \gamma M_0^2 \beta^{-4}[(\gamma+1)M_0^4 - 4\beta^2]\Delta^2/4 + \gamma\beta^{-7}M_0^2[(\gamma+1)^2 M_0^8/32 - (7 + 12\gamma - 3\gamma^2)\,M_0^6/24 + 3(\gamma+1)M_0^4/4 - M_0^2 + 2/3]\Delta^3 + \cdots \qquad (12)$$

where

$$\beta = (M_0^2 - 1)^{1/2}$$

and the Mach number behind the shockwave as a function of the wedge angle is determined as

$$M_2 = \{[M_0^2(6P_j + 1) - 5(P_j^2 - 1)]/[P_j(P_j + 6)]\}^{1/2} \qquad (13)$$

Deceleration Region

In the deceleration region, the Mach number distribution is of the form

$$M = M_2[1 + K(S_a - S_0)/(1 - S_0)]^{-\Phi} \qquad (14)$$

This equation was developed by Wortmann[24] to produce a constant form parameter in the turbulent boundary layer. Notice that the parameters S_0, Φ, and K are quantities that may be varied to produce an infinite number of velocity distributions. In Fig. 5 the variation of Φ is shown to produce a family of Mach number distributions that can be easily converted to pressure coefficient distributions by means of the isentropic gas relationships.

Integrated Performance Results

The pressure distributions on the upper and lower airfoil surface are next integrated numerically for lift and pitching

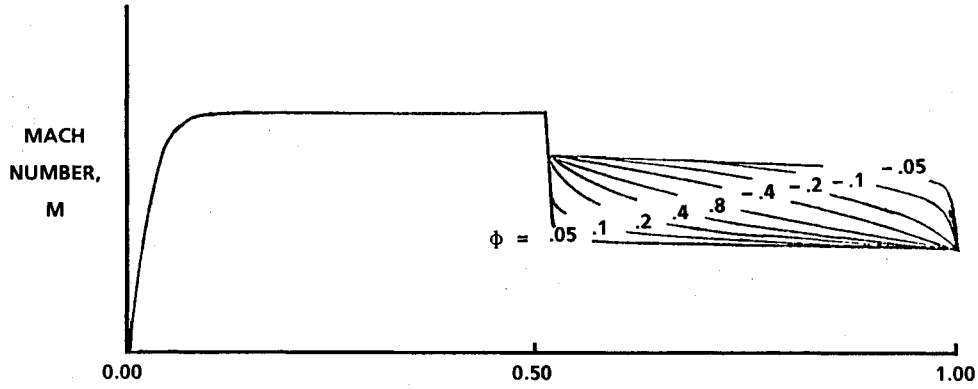

Fig. 5 Effect of Φ on pressure recovery system.

moment on each surface. The friction drag is calculated by means of the Squire-Young drag method in conjunction with the Walz[25] compressible boundary-layer theory. The Walz boundary-layer method is also used to determine if flow separation is likely to occur. Also, a transition location is determined by a method of Eppler and Somers[26] that allows the effective roughness of the surface to be varied. In addition, a capability to set the transition point at or before a given location is available.

Perturbations to the Pressure

The pressure distributions on the upper and lower surface of the airfoil can be defined by five parameters by using this method. However, in the design of airfoil sections with practical leading- and trailing-edge shapes, the simple pressure distribution produced by this method may have to be perturbed slightly to generate realistic input values. One area in which perturbations to the basic pressure distributions may be important is the trailing-edge region. Without viscous effects the pressure at the trailing edge would recover to the stagnation pressure. However, this pressure rise is alleviated by the growth of the boundary layer as it nears the trailing edge of the airfoil. The pressure distribution in this area usually expericnces a small rise. An interactive modification of this pressure can be performed, and the pressure distribution can be modified to produce a realistic trailing-edge pressure distribution. Alternately, a technique such as that of Volpe,[4] discussed previously, may be used to modify these pressure distributions to rigorously provide for a well-posed inverse design problem.

Results

The MGM design procedure has been incorporated into the two-dimensional Navier-Stokes code described previously. The resulting computer program is referred to here as the MGM2D code. In this section we present three sample problems to illustrate application of the design method. Using target pressures obtained from a known "target geometry," the first test case demonstrates that the baseline configuration used to start the design process does not have to be "close" in thickness or camber to the target geometry. The second example is similar to the first but also demonstrates that the MGM2D algorithm can be used to design airfoils even when the baseline leading-edge region requires significant changes. The third example was chosen to solve a specific airfoil design problem where the target pressures were generated with the ADAM system and correspond to certain desired lift and moment coefficients.

Several parameters were held constant for each of the sample problems. The computational C-grid used consisted of 157 nodes in the wraparound or ξ direction (31 of these in the wake region) and 58 nodes in the surface-normal or η direction. The first η = constant grid line was clustered to within 0.00005 chord lengths from the airfoil surface. Also, a locally varying time step was used for both analysis and design, and 50 time steps were used between geometry updates for all design cases.

Design Case 1

For case 1, the MGM2D code was used in the analysis mode to compute the surface pressures corresponding to a NACA 64A010 airfoil at $M_\infty = 0.8$, an angle of attack $\alpha = 0$, and R_e = 6,500,000 based on airfoil chord. Two thousand iterations (time steps) were required to obtain a converged viscous flow solution in which the change in conserved flow variables ΔQ was reduced by five orders of magnitude. It should be noted that for more difficult cases the Navier-Stokes code may require many more iterations (4,000 or more) in the analysis mode to achieve similar convergence levels. However, the convergence characteristics described here are a function of the particular CFD solution procedure used as a basis for the design algorithm and can be affected by a variety of parameters, including grid orthogonality, numerical dissipation, and time-step size.

The calculated C_p values were next used as target pressures for the MGM2D code operated in the design mode. The baseline airfoil used for this case was an RAE2822 section. This airfoil has an aft-loaded camber line and is significantly different in shape from the NACA 64A010 airfoil used to produce the target pressure distribution.

The MGM2D code was run in the design mode for 4,000 iterations with uniform freestream conditions as the initial flowfield solution. That is, a converged flowfield solution for the baseline configuration was not needed to start the design process. The baseline served primarily to set the trailing-edge thickness, which was held constant during the design iterations.

Equations (5) and (6) were evaluated by means of nonuniform physical coordinates for the finite-difference expressions. The values of the user-specified coefficients in these equations were fixed at $F_0 = F_1 = F_2 = 4.0$. Figure 6 compares the final "designed" airfoil and the baseline configuration. To reach the final configuration, values of the maximum residual R_{max} and the average value of the residual over the airfoil surface were both reduced more than two orders of magnitude.

Figure 7 compares the final and target pressure distributions, where the "final" pressures were obtained from an

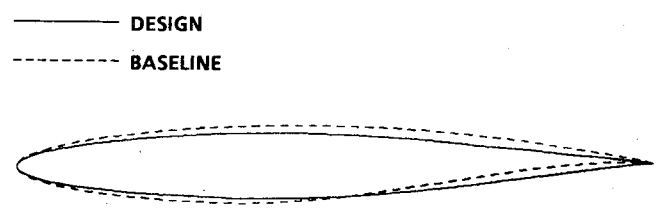

Fig. 6 Comparison of baseline and design airfoil contours for case 1.

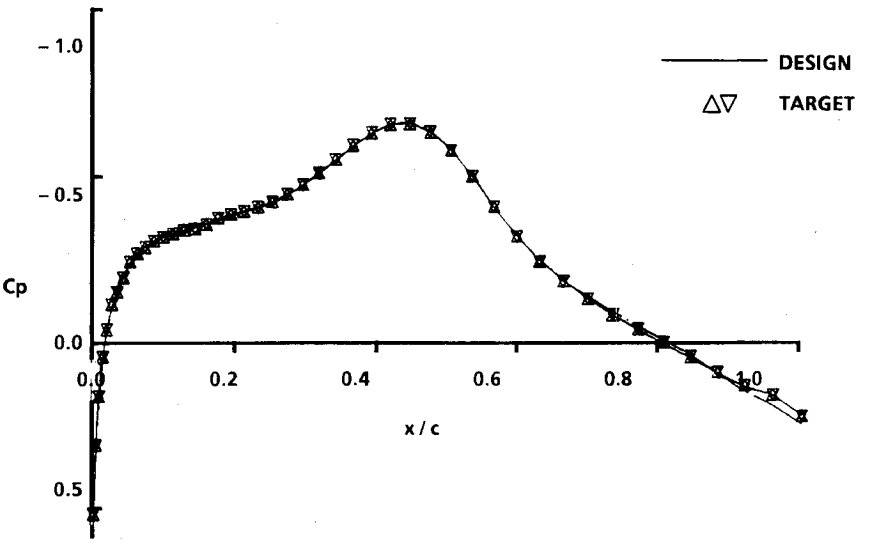

Fig. 7 Comparison of design and target pressure distributions for case 1.

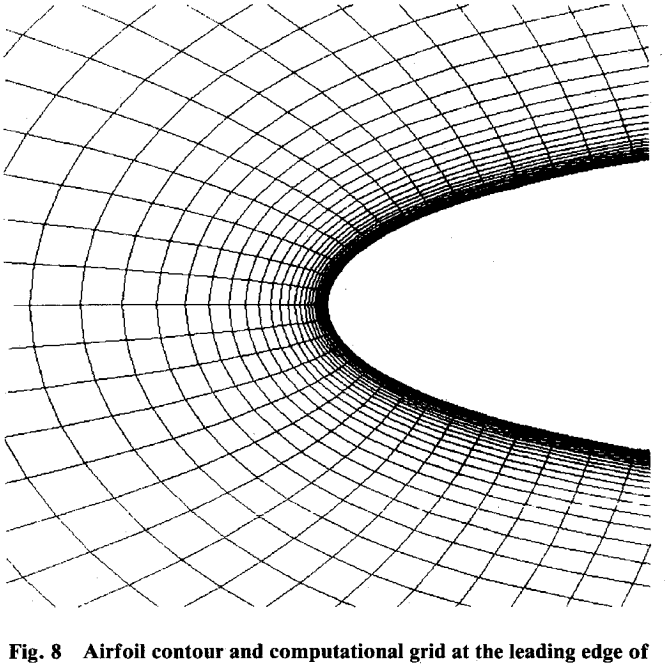

Fig. 8 Airfoil contour and computational grid at the leading edge of the baseline configuration for case 2.

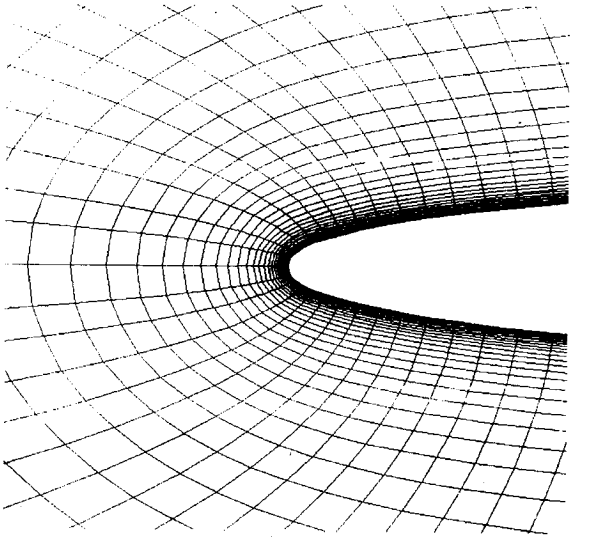

Fig. 9 Airfoil contour and computational grid at the leading edge of the designed configuration for case 2.

analysis of the "designed" airfoil geometry. An analysis of the design configuration verifies that the computational procedure has produced a geometry that matches the target pressures within acceptable tolerances. For this example case, the final design configuration was achieved with not much more computational effort than would have been required to perform a single aerodynamic analysis using the original Navier-Stokes solver.

Design Case 2

The design goal for case 2 was to demonstrate that the MGM2D code can produce airfoils whose pressure distributions required significant modifications to the baseline leading-edge geometry. As in case 1, target pressures were first computed for a known baseline configuration, and then the MGM2D code was used to reproduce the target geometry.

For this example, the target pressures were computed for a NACA 0006 airfoil section at $M_\infty = 0.6$, $\alpha = 0.0$ deg, and $R_e = 1{,}000{,}000$ based on airfoil chord. A NACA 0012 airfoil was used for a baseline configuration. A converged flowfield solution for the NACA 0012 airfoil was used to start the design process. After 4,000 iterations were performed in the design

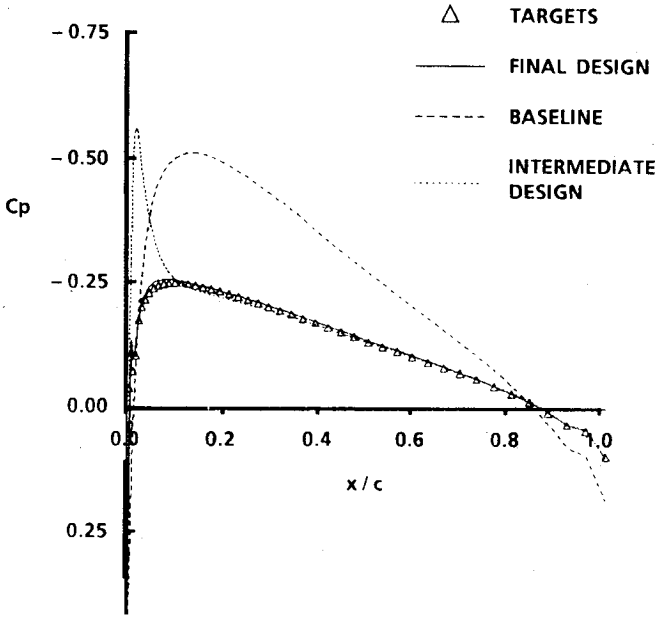

Fig. 10 Comparison of baseline, target, and design and pressure distributions for case 2.

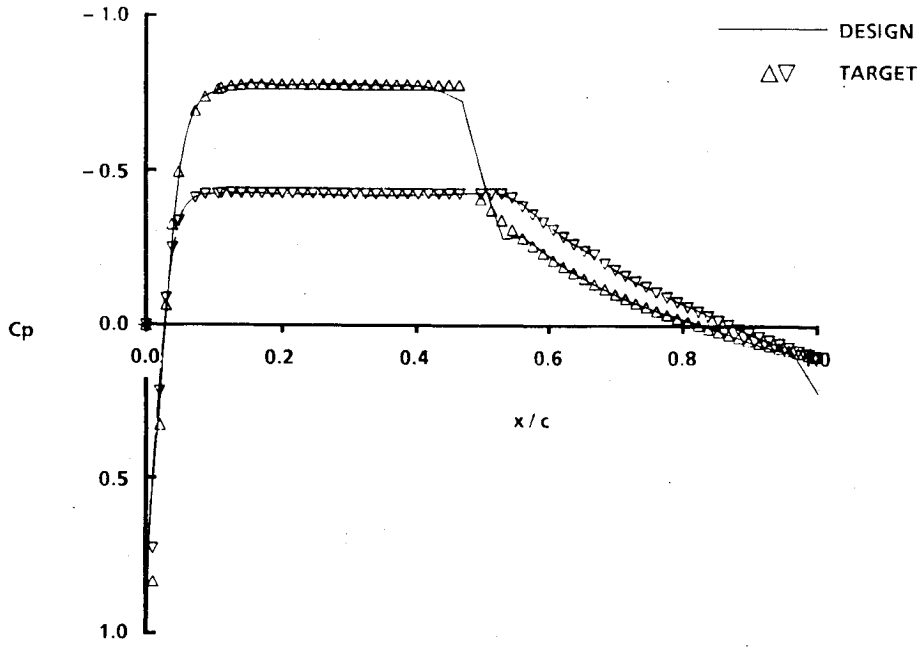

Fig. 11 Comparison of design and target pressure distributions for case 3.

mode, the new airfoil had achieved a reasonable match to the targets everywhere except near the leading edge. After another 1,000 iterations, the value of the maximum residual had dropped by an order of magnitude.

Results for this sample problem are given in Figs. 8–10. Figure 8 shows the leading-edge region of the NACA 0012 baseline airfoil, whereas Fig. 9 illustrates the leading-edge region of the designed airfoil. Finally, Fig. 10 compares the upper-surface pressure coefficient distributions for the target pressures, the design pressures after 4,000 iterations, and the final design pressures after an additional 1,000 iterations. Although case 2 is a relatively simple design problem, it demonstrates that the present numerical procedure can produce successful airfoil designs even when large changes are required to a given baseline shape. For this case a 50% reduction in maximum t/c and corresponding large changes in leading-edge radius were achieved.

Design Case 3

For case 3, an airfoil was to be designed with a maximum thickness of approximately 11% of chord, a design lift coefficient of 0.128, a nose-up pitching moment coefficient of 0.0078 at a Mach number of 0.78, a Reynolds number of 4.2×10^6 based on airfoil chord, and a drag divergence Mach number greater then 0.78 at the design lift coefficient. The ADAM system was used to find pressure distributions that would satisfy these requirements and yield low drag coefficients.

The problem posed by case 3 represents a robust test of the MGM2D code for two reasons. First, the target pressure distribution incorporates a medium strength shockwave on the airfoil upper surface. In addition, the target pressures selected are flat "rooftop" type distributions ($\partial C_p/\partial x = 0$) over large portions of the upper and lower surfaces of the airfoil. This target C_p distribution is plotted in Fig. 11 as upper (∇) and lower (Δ) surface symbols.

The starting configuration used for this problem was a symmetrical NACA 64A010 airfoil section. As in case 1, this design problem used an impulsive start from uniform freestream conditions.

Approximately 12,000 iterations were used to produce an airfoil shape that gave a reasonably close match to the target pressure distribution. The sign was generated with two different sets of coefficients F_0, F_1, and F_2. For the initial 4,000 iterations, values of these coefficients were set at $F_0 = F_1 = F_2 = 4.0$. For the second 4,000 iterations, the design process was slowed down slightly by increasing the values of these coefficients to $F_0 = F_1 = F_2 = 10.0$. This has the effect of further reducing the amount of the correction ΔY_i applied to the airfoil surface. The final 4,000 iterations used values of $F_0 = F_1 = F_2 = 4.0$.

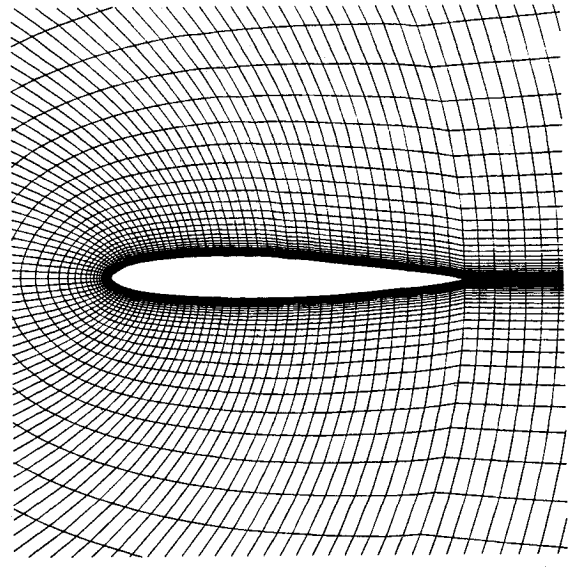

Fig. 12 Design airfoil shape and computational grid for case 3.

The airfoil pressures resulting from the final design geometry are also shown in Fig. 11, whereas the design airfoil contour and computational grid are shown in Fig. 12. The final designed airfoil lift and moment coefficients obtained are 0.1200 and 0.007, respectively. These results reflect a 6% difference in lift coefficient and 10% difference in moment coefficient. An examination of Fig. 11 shows that while good agreement has been obtained between pressures on the designed airfoil and the target pressure distributions over the majority of the airfoil surface, the region of greatest differences occurs near the airfoil's trailing edge. A target pressure distribution with more pressure recovery allowed at the trailing edge, a modification subsequently added to the ADAM

system, has been used to produce an airfoil design with a much closer match to the targets in this trailing-edge region.

Concluding Remarks

The MGM design procedure has been incorporated into an existing Navier-Stokes code. The present method is relatively efficient in that it does not significantly increase the computational effort required to obtain airfoil designs above that normally required to use the Navier-Stokes code in the analysis mode. Experience with this method has shown that many design problems can be solved for the same computational effort as that required for a single Navier-Stokes analysis. However, because of the computer resource requirement, any Navier-Stokes-based design method would prove most beneficial when used in combination with other, lower order methods. For example, an initial airfoil shape designed with a lower cost FPE method may prove to be an excellent starting configuration for a higher order design approach. Used in this manner, the present Navier-Stokes inverse design method should then be able to account for viscous flowfield phenomena that may not be detected or predicted accurately enough by other methods based on FPE or Euler solution procedures.

Acknowledgments

This research was supported by the Independent Research and Development program at Bell Helicopter Textron, Inc. The original Navier-Stokes code used in this work was developed with support of the U. S. Army Research Office CERWAT program. The authors also thank Cray Research, Inc., for providing computer resources used in developing and validating the computational design method described in this paper. They offer special thanks to J. Ahnert, V. Stack, and H. Gonzalez of Cray Research, Inc., Dallas District.

References

[1]Sloof, J. W., "Computational Methods for Subsonic and Transonic Aerodynamic Design," AGARD Rept. 712, 1983.

[2]Lores, M. E., and Smith, P. R., "Supercritical Wing Design Using Numerical Optimization and Comparisons with Experiment," AIAA Paper 79-0065, Jan. 1979.

[3]Weed, R. A., Anderson, W. K., and Carlson, L. A., "A Direct-Inverse Three-Dimensional Transonic Wing Design Method for Vector Computers," AIAA Paper 84-2156, Aug. 1984.

[4]Volpe, G., "Inverse Design of Airfoil Contours: Constraints, Numerical Method, and Applications," AGARD-CP-463, May 1989, pp. 4.1-4.18.

[5]Takanashi, S., "Iterative Three-Dimensional Transonic Wing Design Using Integral Equations," *Journal of Aircraft,* Vol. 22, No. 8, 1985, pp. 655-660.

[6]Mani, K. K., "Design Using Euler Equation," AIAA Paper 84-2166, Aug. 1984.

[7]Giles, M. B., and Drela, M., "Two-Dimensional Transonic Aerodynamic Design Method," *AIAA Journal,* Vol. 25, No. 9, 1987, pp. 1199-1205.

[8]Risk, M. H., "Applications of Single Cycle Optimization Approach to Aerodynamic Design," AIAA Paper 84-2165, Aug. 1984.

[9]Hirose, N., Takanashi, S., and Kawai, N., "Transonic Airfoil Design Procedure Utilitizing a Navier-Stokes Analysis Code, *AIAA Journal,* Vol. 25, No. 3, 1987, pp. 353-359.

[10]Garabedian, P., and McFadden, G., "Design of Supercritical Swept Wings," *AIAA Journal,* Vol. 20, No. 3, 1982, pp. 289-291.

[11]Malone, J. B., Vadyak, J., and Sankar, L. N., "A Technique for the Inverse Aerodynamic Design of Nacelles and Wing Configurations," AIAA Paper 85-4096, Oct. 1985 (see also *Journal of Aircraft,* Vol. 24, No. 1, 1987, pp. 8-9).

[12]Hazarika, N., "An Efficient Inverse Method for the Design of Blended Wing-Body Configurations," Ph.D. Thesis, Georgia Institute of Technology, Atlanta, GA, June 1988.

[13]Malone, J. B., Narramore, J. C., and Sankar, L. N., " An Efficient Airfoil Design Method Using the Navier-Stokes Equations," AGARD-CP-463, May 1989, pp. 5.1-5.18.

[14]Birckelbaw, L., "Inverse Airfoil Design Using the Navier-Stokes Equations," AIAA Paper 89-2202, July-Aug. 1989.

[15]Sankar, L. N., and Tang, W., "Numerical Solution of Unsteady Viscous Flow Past Rotor Sections," AIAA Paper 85-0129, Jan. 1985.

[16]Huff, D. L., and Sankar, L. N. "Analysis of Viscous Transonic Flow Over Airfoil Sections," AIAA Paper 87-0420, Jan. 1987.

[17]Beam, R. M., and Warming, R. F., "An Implicit Factored Scheme for the Compressible Navier-Stokes Equations," *AIAA Journal,* Vol. 16, No. 4, 1978, pp. 393-401.

[18]Baldwin, B., and Lomax, H., "Thin-Layer Approximation and Algebraic Model for Separated Turbulent Flow," AIAA Paper 78-0257, Jan. 1987.

[19]Davis, W. H., "Technique for Developing Design Tools from Analysis Methods of Computational Aerodynamics," AIAA Paper 79-1529, July 1979.

[20]Anderson, D. A., Tannehill, J. C., and Pletcher, R. H., *Computational Fluid Mechanics and Heat Transfer,* McGraw-Hill, 1984.

[21]Malone, J. B., "Subsonic Panel Method for Iterative Design of Complex Aircraft Configurations," *Journal of Aircraft,* Vol. 19, No. 10, 1981, pp. 820-825.

[22]Narramore, J. C., and Yeary, R. D., "Airfoil Design and Analysis Using an Information Systems Approach," AIAA Paper 80-1444, July 1980.

[23]Yoshihara, H., "Transonic Viscous Interactions," *AIAA Professional Study Series, Seminar Notebooks,* Snowmass, CO, July 1980.

[24]Wortmann, F. X., "A Contribution to the Design of Laminar Profiles for Gliders and Helicopters," German Ministry of Aviation Translations TIL/T4903, Sept. 1960.

[25]Walz, A., *Boundary Layers of Flow and Temperature,* edited and translated by H. J. Oser, Cambridge, MA, 1969, pp. 262-270.

[26]Eppler, R., and Somers, D. M., "A Computer Program for the Design and Analysis of Low-Speed Airfoils," NASA TM-80210, Aug. 1980.